Single Amino Acid Mutation Decouples Photochemistry of the BLUF Domain from the Enzymatic Function of OaPAC and Drives the Enzyme to a Switched-on State

Jinnette Tolentino Collado [1,#], Emoke Bodis [2,#], Jonatan Pasitka [2], Mihaly Szucs [2], Zsuzsanna Fekete [2], Nikolett Kis-Bicskei [2], Elek Telek [2], Kinga Pozsonyi [2], Sofia M. Kapetanaki [2], Greg Greetham [3], Peter J. Tonge [1,*], Stephen R. Meech [4,*] and Andras Lukacs [2,*]

*1 - **Department of Chemistry,** Stony Brook University, New York 11794, United States*
*2 - **Department of Biophysics,** Medical School, University of Pecs, Szigeti str. 12, 7624 Pecs, Hungary*
*3 - **Central Laser Facility,** Research Complex at Harwell, Rutherford Appleton Laboratory, Didcot OX11 0QX, UK*
*4 - **School of Chemistry,** University of East Anglia, Norwich, NR4 7TJ, UK*

Correspondence to Peter J. Tonge, Stephen R. Meech and Andras Lukacs:*Corresponding authors. *peter.tonge@stonybrook.edu (P.J. Tonge), s.meech@uea.ac.uk (S.R. Meech), andras.lukacs@aok.pte.hu (A. Lukacs)*
https://doi.org/10.1016/j.jmb.2023.168312
Edited by John Kennis

Abstract

Photoactivated adenylate cyclases (PACs) are light-activated enzymes that combine a BLUF (blue-light using flavin) domain and an adenylate cyclase domain that are able to increase the levels of the important second messenger cAMP (cyclic adenosine monophosphate) upon blue-light excitation. The light-induced changes in the BLUF domain are transduced to the adenylate cyclase domain via a mechanism that has not yet been established. One critical residue in the photoactivation mechanism of BLUF domains, present in the vicinity of the flavin is the glutamine amino acid close to the N5 of the flavin. The role of this residue has been investigated extensively both experimentally and theoretically. However, its role in the activity of the photoactivated adenylate cyclase, OaPAC has never been addressed. In this work, we applied ultrafast transient visible and infrared spectroscopies to study the photochemistry of the Q48E OaPAC mutant. This mutation altered the primary electron transfer process and switched the enzyme into a permanent 'on' state, able to increase the cAMP levels under dark conditions compared to the cAMP levels of the dark-adapted state of the wild-type OaPAC. Differential scanning calorimetry measurements point to a less compact structure for the Q48E OaPAC mutant. The ensemble of these findings provide insight into the important elements in PACs and how their fine tuning may help in the design of optogenetic devices.

Introduction

OaPAC is a photoactivated adenylate cyclase (PAC) discovered recently in the cyanobacteria *Oscillatoria acuminata* that translates a blue-light signal into the production of cyclic adenosine monophosphate (cAMP).[1] OaPAC is a homodimer of a 366-aa protein comprising an N-terminal BLUF (blue-light sensing using FAD) domain and a C-terminal class III adenylyl cyclase (AC) domain. The basal activity of OaPAC is very low under dark conditions, but under light conditions it is stimulated up to 20-fold, making OaPAC a very good candidate for optogenetic applications.[1]

PACs have captured the interest of biologists in the past two decades after the discovery of

EuPAC, the first member of the family found in the unicellular flagellate, *Euglena gracillis*, in which the step-up photophobic response is mediated by the cyclase activity.[2] In the majority of PACs the light dependent production of cAMP is controlled by a BLUF domain located at the N-terminal of the protein.[2] PACs exploit the photochemistry of the BLUF domain to transmit a light-induced downstream signal that enhances the cAMP levels.[3–4] All BLUF proteins work using the same elegant mechanism: blue light absorption of the flavin leads to a rearrangement of the hydrogen bond network around the flavin and this primary structural change propagates through the protein leading to intramolecular conformational changes at the C-terminal that regulates the activity of the protein or can even control interprotein interactions.[5–10] In our earlier work, using time-resolved multiple probe spectroscopy (TRMPS) we were able to follow the propagation of the signal in the BLUF domain of Activator of the Photopigment and pucA (AppA) by monitoring the structural changes occurring in the β-sheet within 20 μs of light absorption.[11]

The photochemistry of BLUF domains depends on the conserved amino acid residues around the isoalloxazine ring[12–17] (Figure 1). A close-lying tyrosine (conserved in all BLUF domains) serves as both an electron and a proton donor. Another key amino acid residue which is also conserved in all BLUF domains is the glutamine residue close to the N5 atom of the flavin. The role of glutamine (Q48 in OaPAC, Q63 in AppA, Q50 in PixD) in the photoactivation of BLUF domain proteins has been extensively investigated, as it was observed that it is necessary for transmitting the structural change from the BLUF domain towards the C-terminal part of the protein.[16,18–20] Replacement of this amino acid residue resulted in the loss of the characteristic spectral red-shift observed in BLUF domain proteins upon blue light irradiation.[21–22] The group of Bauer was the first to replace the glutamine residue Q63 in AppA with a glutamic acid and they have observed a ~3 nm red shift (from 446 nm to 449.5 nm) of the S_0-S_1 transition of the flavin in the Q63E AppA mutant.[21] Based on this observation and fluorescence spectroscopy experiments they proposed that the Q63E AppA mutant is in lit mode. An early model, deduced from the first crystal structure of AppA,[23] proposed that the glutamine side chain rotates after photoexcitation. Based on transient infrared experimental data and quantum chemical calculations it was proposed that a photoinduced keto-enol tautomerization of the close glutamine (Q63) to the N5 atom of flavin leads to the ultrafast reorganization of the hydrogen bond network.[16,24] Quantum chemical calculations show that the driving force for this is an electron transfer reaction[25–26] mediated by structural relaxation where Y6 is the primary electron donor, but W90 can donate an electron as well, as in the WT protein we observed the formation of the anionic flavin radical ($FAD^{\bullet-}$) at early times after excitation but only the neutral flavin radical was formed in the W90F mutant.[4] Based on our time resolved infrared (TRIR) and visible transient absorption (TA) measurements[4] we proposed that the primary photochemistry of OaPAC is the following: tyrosine Y6 gives an electron and a proton at the same time (concerted forward proton -coupled electron transfer, PCET) to the oxidized flavin to form the semiquinone flavin ($FADH^{\bullet}$) in ~24 ps. In less than 200 ps, $FADH^{\bullet}$ decays to the signalling state of the flavin via a reverse electron and proton transfer to the tyrosine Y6. This signalling state is characterized by the well-known red-shift of the S0-S1 transition and of the C4 = O carbonyl stretch of the flavin in the absorption and infrared spectra, respectively. The flavin remains in this signalling state for ~5 s, and the ATP- cAMP conversion happens during this time. However, there is an open question on the nature of the hydrogen bond reorganization around the flavin and how this rearrangement is transduced to the AC domain of OaPAC.

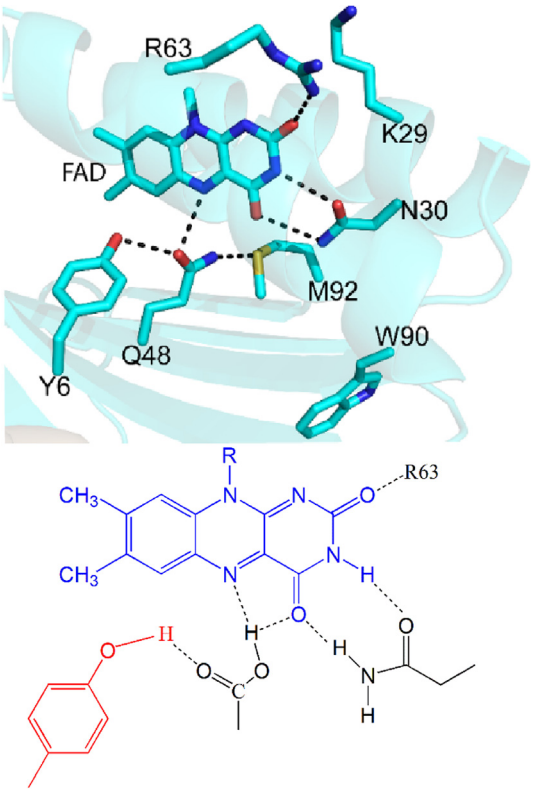

Figure 1. A) Environment of FAD in OaPAC (pdb:4yus) showing the residues involved in the hydrogen bond network around the flavin. Glutamine is hydrogen bonded to the flavin, the tyrosine and the methionine before excitation. B) Possible orientation of E48 and hydrogen bonds to the flavin.

It should be pointed out that the radical intermediate states mentioned above for the flavin and the tyrosine residue have been identified in

some BLUF domains (but not in AppA), by their characteristic markers in ultrafast visible and infrared measurements[4,25–29] whereas the forward PCET step has been reported to be sequential in PixD.[25–27] Regardless of the sequence of the PCET reaction (concerted or sequential), the conserved glutamine residue is considered crucial for the propagation of the signal from the BLUF domain to the effector domain with the keto-enol tautomerization being the focus of many experimental and theoretical studies in AppA and PixD.[22,28–33] In particular, very recently Hontani et al.[34] revisited the tautomerization models in PixD by means of femtosecond stimulated Raman spectroscopy (FSRS), isotope labelling and computational methods and they revisited the models proposed (in the case of AppA) for the light activation. The authors concluded that the Anderson[13,35] model which proposed the rotation of this specific glutamine residue cannot be used to explain the experimental data. They also proposed that the Sadeghian/Stelling[16,36] model which proposed to form a tautomer in the light adapted state but without rotating its side chain does not fit their observation neither. Hontani et al. concluded that after photoexcitation glutamine tautomerizes to the imidic form which is followed by a sidechain rotation to form the light adapted state.

In a recent ultrafast absorption study Chen et al.[37] have studied bidirectional proton relay using the triple OaPAC BLUF mutant Y6WQ48EW90F and have decoupled the forward electron transfer and the proton transfer from tyrosine Y6 to the flavin. The results obtained allowed them to propose a Grotthus mechanism[38]– a proton transfer along a hydrogen bond – taking place during the protonation of the flavin by Q48E.

Despite the intense interest in the role of the glutamine residue on BLUF domains, there are no studies addressing the potential effect of the glutamine mutation on the effector domain in BLUF and PAC proteins. The studies mentioned above have been performed on the BLUF domains and not on the full-length proteins. To investigate the implications of the glutamine residue on the enzymatic activity of OaPAC, we have studied the functional dynamics of the full-length Q48E OaPAC mutant using ultrafast transient visible and infrared spectroscopies and contrasted them with the functional dynamics of the wild-type full-length OaPAC. The glutamine to glutamic acid mutation is an interesting one as it removes the possibility of either an asymmetry in the rotation or the formation on the imine tautomer while offering the potential of retaining the H-bond structure around the flavin ring.

As in OaPAC the photosensor domain and the effector domain are part of the same protein – contrary to the AppA-PpsR complex – it was a straightforward idea to study the effects of this mutation on the functional activity of the protein.

As expected, the Q48E mutation indeed suppresses photoactivity. We have also shown that it significantly affects the structure of the enzyme, as indicated by differential scanning calorimetry measurements. Our findings support a proton coupled electron transfer pathway in the Q48E OaPAC mutant. In addition, enzymatic assays suggest that replacement of the glutamine by the glutamic acid locks the protein in a 'switched-on' state that decouples the adenylate cyclase domain from the BLUF domain and converts ATP to cAMP in a light- independent manner. Comparisons with the analogous mutation in $PixD_{BLUF}$ (Q50E) are made and the implications of our results on the engineering of PACs for optogenetic applications are discussed.

Results and Discussion

The absorption spectrum of the Q48E OaPAC mutant shows a significant difference to the absorption spectrum of the wild-type enzyme, with the maximum of the visible flavin absorption attributed to the S_0-S_1 π-π^* transition of the isoalloxazine moiety[39] at 448 nm red-shifted by 6 nm compared to the wild-type (Figure 2). Since the characteristic dark to light 10–15 nm red-shift of the specific flavin transition in BLUF domains originates from a hydrogen bond rearrangement around the flavin, it can be postulated that the observed 6 nm red-shift of the absorption maximum in the Q48E OaPAC mutant arises from a mutation induced change in the hydrogen bond network around the flavin. It is worth mentioning that the analogous Q63E mutation in $AppA_{BLUF}$ resulted in a smaller red-shift (3 nm).[22] Similar to the Q63E AppA mutant, blue-light irradiation of the Q48E OaPAC mutant does not result in a further red-

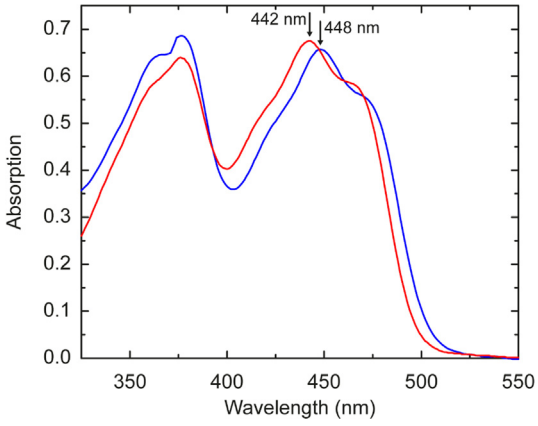

Figure 2. Absorption spectra of the dark-adapted states of the wild-type OaPAC (red line) and the Q48E OaPAC mutant (blue line). The absorption maximum is red shifted in the Q48E mutant suggesting a change in the surrounding hydrogen bonding network of the flavin.

shift of the maximum absorption of the flavin, indicating that the Q48E OaPAC mutant is photoinactive.

Transient absorption measurements

To characterize the early steps of the photochemistry of the Q48E OaPAC mutant, we applied ultrafast transient absorption spectroscopy. Transient absorption spectra of BLUF domain proteins are dominated by the spectral properties of the flavin chromophore; the transient absorption spectrum has three salient features: a negative ΔA (called bleach) in the spectral region (400–500 nm) where the flavin absorbs (S_0-S_1 transition), a positive peak (excited state absorption, ESA) near 500 nm and a broad negative band at > 530 nm attributed to stimulated emission (SE). Global analysis of the data, assuming a sequential kinetic model revealed a heterogeneous decay with three decay constants (1 ps, 23 ps, 311 ps). The transient absorption spectra of the Q48E (Figure 3(A)) do not show any obvious components which can be assigned to the formation of radical intermediates which have distinct spectral features (see Figure S5, $FADH^{\bullet}$ has a broad absorption in the 500–700 nm range, $FAD^{\bullet-}$ has a distinct peak at 400 nm). The evolution associated difference spectra (EADS, Figure 3(B)) also did not resolve a clear radical intermediate although spectral modelling of the 311 ps component show the presence of the $FADH^{\bullet}$ species (see Fig S5. C) This may reflect an overlap with the SE and ESA or that any radical population is low due to kinetic considerations; the spectra of the radical species have been proven elusive in other BLUF domains. However, the fact that the excited FAD* state decays in hundreds of picoseconds points to an effective quenching which could be the result of an electron transfer to the excited flavin, otherwise FAD* would have a longer lifetime (~4 ns).[28]

Transient infrared absorption measurements

To obtain a more detailed picture on the nature of the flavin intermediates as well as of the changes occurring in the protein vibrational spectra following blue-light excitation, we performed time-resolved infrared spectroscopy (TRIR). Figure 4(A) shows the temporal evolution of the TRIR spectra of the dark-adapted state of the Q48E OaPAC mutant after blue-light excitation. The most salient features of the TRIR spectra observed at 10 ps after excitation are related to the flavin vibrational modes and are similar to those observed in the wild-type OaPAC.[4] The intense bleach at 1547 cm^{-1} and the weaker one at 1581 cm^{-1} are well known flavin adenine dinucleotide (FAD) ring modes.[29–33] The most significant differences compared to the TRIR spectra of wild-type OaPAC (Figure S2) are the negative peak observed at 1730 cm^{-1}, the positive peak at 1704 cm^{-1} and a negative bleach around 1690 cm^{-1}. In the wild-type enzyme a bleach is observed at 1704 cm^{-1} assigned to the bleached FAD ground state carbonyl. This significant difference at the higher frequencies is the result of a mutation-induced change in the hydrogen bond network around the flavin as explained below. In our earlier work[22] on the analogous Q63E mutation in AppA we showed using isotope labelling that the new bleach (at 1724 cm-1 in $AppA_{BLUF}$) does not originate from a flavin vibrational mode but from the side chain of the glutamic acid. Moreover, this high-frequency band (1724 cm^{-1} in Q63E AppA and 1730 cm^{-1} in Q48E OaPAC) is observed in the expected absorption range of protonated carboxylic acids (1700–1770 cm^{-1})[40–44] and therefore can be assigned to

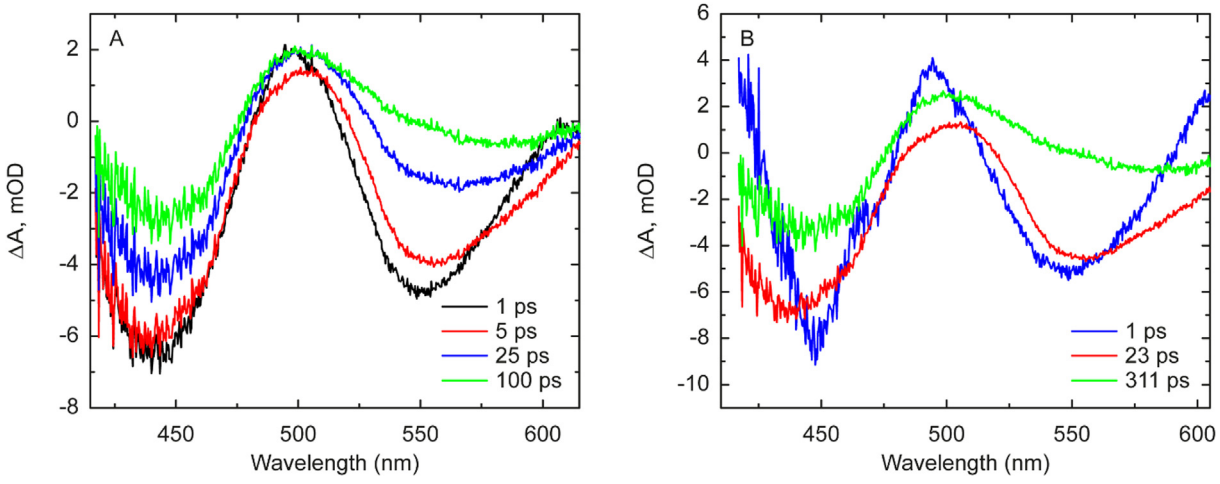

Figure 3. A) Comparison of transient absorption spectra of the Q48E mutant at the indicated time delays. The spectra are dominated by a bleach around 450 nm, excited state at ~500 nm and simulated emission in the ~520–570 nm region B) EADS spectra obtained after the global analysis show a heterogeneous decay of the excited state.

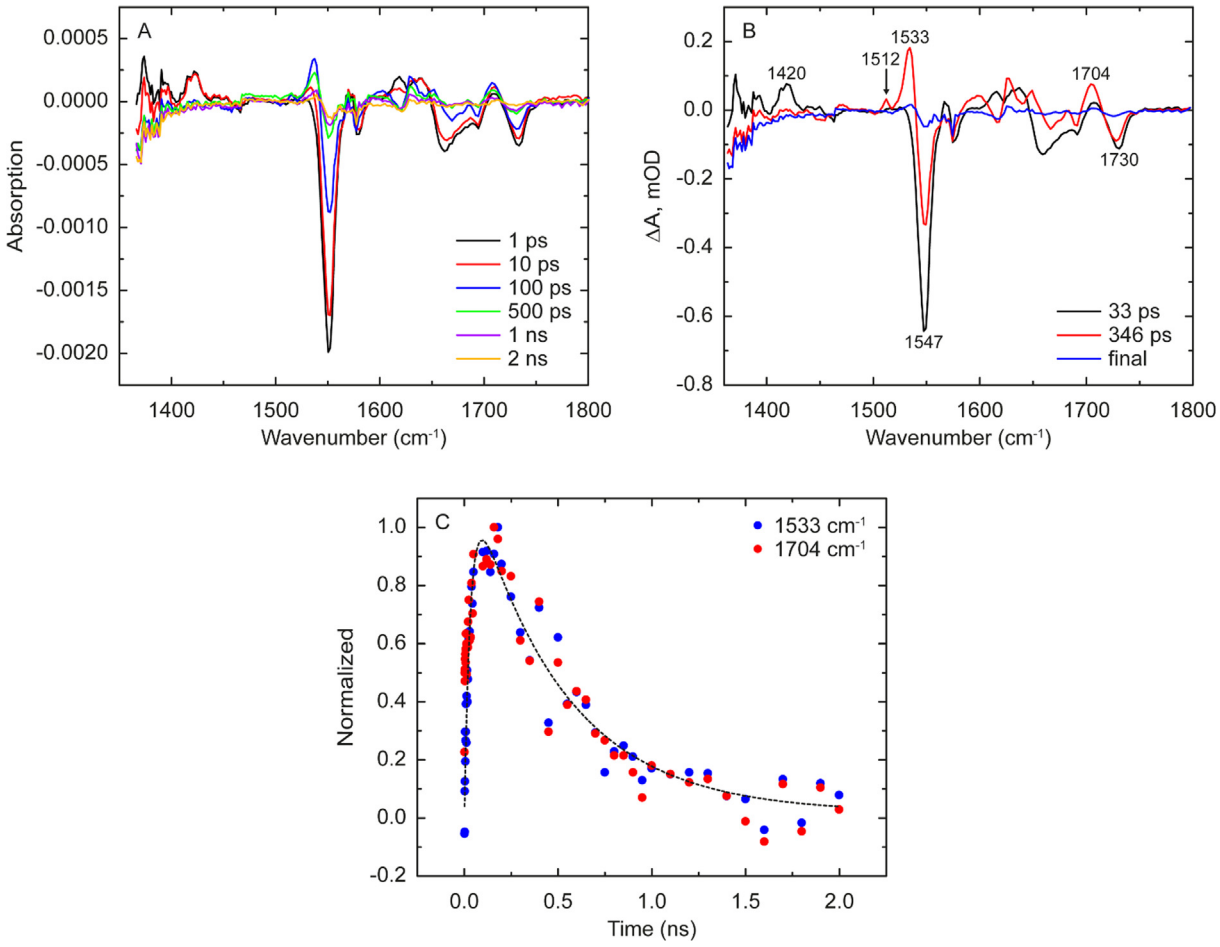

Figure 4. A) Transient infrared spectra of the Q48E mutant at the indicated time delays B) EADS spectra from the global analysis performed on the transient infrared data C) Kinetics observed at 1533 cm^{-1} and 1704 cm^{-1} (the sign of the latter is inverted for comparison).

the vibrational mode of a protonated carboxylic acid side chain of the glutamic acid. The presence of the ~1690 cm^{-1} bleach indicates that the carbonyl at the C4 atom of FAD forms a hydrogen bond with the glutamic acid already at the moment of excitation (see Fig 1B). The exact same peak is formed in the wild-type OaPAC 184 ps after excitation and has been assigned to a downshifted C4 = O group (1704 cm^{-1} in the ground-state) of the glutamine residue due to an additional hydrogen bond to it.[4] The origin of the positive 1704 cm^{-1} peak is more complex: it could be assigned to the vibration of the protonated carbonyl of E48 but can partially arise from the C4 = O carbonyl and is discussed in more detail bellow.

The EADS of the TRIR for the Q48E mutant are shown in Figure 4(B). Assuming a sequential model, global analysis of the TRIR data reveals two components with lifetimes 33 ps, 346 ps and a third constant component with an infinite lifetime. The first EADS spectrum can be assigned to the difference spectrum of the oxidized flavin; the 1420 cm^{-1} peak is a vibrational marker of the flavin S_1 excited state.[17] Comparison of the relaxation of the excited state (1420 cm^{-1}) and the ground state recovery observed 1547 cm^{-1} (Figure S1(A)) shows that the time constant of the excited state decay is significantly faster than that of the ground state recovery, pointing to the formation of intermediates during the ground state recovery process.[17] These can be identified as radical intermediates in EADS2, where one can observe the formation of three distinct peaks at 1512 cm^{-1}, 1533 cm^{-1} and 1704 cm^{-1}. The appearance of the peak at 1533 cm^{-1} suggests the formation of a neutral flavin radical $FADH^{\bullet}$ in 33 ps, as this peak is a known vibrational marker of the neutral flavin radical.[4,45] The 1512 cm^{-1} peak forms with the same time constant (Figure S1(B)) and we have previously assigned this to a vibrational mode of the neutral tyrosyl,[4,45] its formation with the same time constant indicates the formation of the $Y6^{\bullet}$ radical simultaneously with the formation of the $FADH^{\bullet}$ radical.

The kinetics of the 1533 cm^{-1} peak (the protonation of the flavin, $FADH^{\bullet}$) share the same time constant (~33 ps) with the rise of the 1704 cm^{-1} mode (Figure 4(C)).

Based on theoretical calculations on Slr 1694 (PixD)[26] a double proton transfer was proposed for the photoactivation of OaPAC[4,46–47]: after photoexcitation the tyrosine gives an electron to the flavin and a proton to the glutamine (Q48) and the glutamine protonates the flavin forming the FADH• intermediate. This concerted PCET mechanism differs from the sequential mechanism observed for the Y6WW90FQ48E OaPAC mutant reported by Chen et al..[37] In their study, they assigned a fast proton transfer (3.8 ps in water) from the glutamic acid to the anionic flavin radical, followed by a slower proton transfer (336 ps in water) from the tryptophan cation radical to the deprotonated glutamic acid. This difference is not surprising, as the pK_a of the tyrosine cation radical is significantly lower (∼-2)[48] than that of the tryptophan cation radical (∼4),[49] justifying a faster deprotonation step for the tyrosine. It should be pointed out that the fast deprotonation of the tyrosine is the reason that the formation of the tyrosine cation radical has been observed by ultrafast spectroscopy in only a few systems.[50–52] The 346 ps EADS shows the radical recombination reaction to largely recover the original ground state.

The two TRIR EADS must be compared to the three from the TA, requiring an assignment of the additional 1 ps component appearing only in the latter. This could indicate a vibrational relaxation in the excited state as the ∼5000 cm^{-1} excess energy in the 400 nm excitation is dissipated, modifying the shape of the transient electronic spectra. Such a relaxation of the hot electronically excited state need not have a signature in the transient IR spectra, where in any case the excess energy is less due to the 450 nm excitation used. Alternatively, an ultrafast charge separation and recombination reaction could occur in a subpopulation of the protein that is not detected in TRIR. Both calculation and experiment in other BLUF domains point to a distribution of ground state structures and inhomogeneous decay kinetics.[6,53–54] Thus, a population with exceptionally fast charge separation and recombination may exist. Such an unproductive photocycle might not be resolved in the lower time resolution and signal to noise of TRIR.

For the remaining two EADS, there is reasonable agreement between the two time constants recovered (33 and 346 ps from TRIR and 23 and 311 ps in TA). However, even here the two components are not obviously due to the same underlying processes. For example the 33 ps TRIR appears to show complete decay of the FAD* state (1420 cm-1). However the longer lives EADS in TA data shows both SE and ESA components, consistent with some longer lived population in FAD*. Similarly, the TRIR EADS at 1547 cm^{-1} shows significant repopulation of the ground state FAD_{ox} (which will also contribute to refilling 1704 cm^{-1}). This is not expected if FAD* decay is exclusively to the FADH• intermediate, with ca 300 ps lifetime. Moreover, the TA data did not clearly show the presence of radical intermediates. Thus, although the TRIR data can be fit with a single intermediate sequential kinetics, the EADS from TA and TRIR indicate an underlying complexity, which we ascribe to inhomogeneity in the excited state dynamics, as has been observed in other BLUF domains.[12,17,22] In that case the 33 ps decay of FAD* is likely better understood as the mean of a distribution of excited state decay times, some of which lead to FADH• while others are unproductive and recover the ground state or leave FAD* to decay on the longer time scale (contributing to SE and ESA in the TA data and the long lived ground state bleach in TRIR). We suggest this kinetic inhomogeneity reflects the existence of multiple ground state structures around the flavin, consistent with a dynamic flavin binding site at room temperature.

To complement the study of Q48E OaPAC we also investigated the effect of the replacement of the analogous glutamine with a glutamic acid residue in the photochemistry of the BLUF protein Slr 1694 (PixD); Figure S3 shows the EADS spectra of this Q50E PixD mutant. The TRIR spectra of the Q50E mutant also show the presence of the 1730 cm^{-1} mode (indicating that the same hydrogen bonding happens as in Q48E OaPAC) as well as the vibrational modes assigned to the neutral tyrosine and flavin radicals. Global analysis revealed two components with lifetimes 5 ps and 49 ps and a third constant component with an infinite lifetime describing the kinetics after blue-light excitation of the flavin. The neutral flavin radical is formed within ∼5 ps (Figure S3). The second EADS shows the characteristic peaks at 1513 cm^{-1} and 1531 cm^{-1} which correspond to vibrational markers of the tyrosine neutral radical and the neutral flavin radical ($FADH^{\bullet}$), respectively. The Q50E mutation changes significantly the photochemistry of PixD, as in the wild-type protein four components with lifetimes 2.5 ps, 20 ps, 110 ps and 525 ps are required to portray the dynamics.[27] The photoactivation process in the wild-type protein is sequential, with the formation of the anionic flavin radical followed by the stabilization of the neutral flavin radical.[27] In contrast, in the Q50E PixD mutant the formation of the FADH• and tyrosine neutral radicals are formed with the same time constant within 5 ps (Figure S3). This is similar to the mechanism seen in the Q48E OaPAC mutant. These results suggest that the specific mutation in PixD shifts the photochemistry in the direction of a concerted PCET (proton coupled electron transfer) and results in a loss of photoactivity in the protein.

Measurement of ATP-cAMP conversion

We examined the impact of the Q48E mutation on the ability of the AC domain to convert ATP to

cAMP. The ATP to cAMP conversion rate in the Q48E OaPAC mutant was measured using a spectrophotometric coupled assay as described in the experimental section. Figure 5(A) shows the enzymatic activity of 2 μM wild-type OaPAC and the 2 μM Q48E mutant as a function of ATP concentration. The maximal velocity of the conversion rate is ~1.5 times higher in the Q48E mutant (0.095 ± 0.003 mM/min) relative to the WT protein (0.064 ± 0.001 mM/min) whereas the concentration of the half-maximal velocity (K_M) is ~0.6 lower. The catalytic constant (k_{cat}) which gives the number of substrate molecules that can be converted to cAMP by the enzyme per unit time is ~1.5 times higher in the Q48E OaPAC (47.5 ± 0.2 1/min) than in the wild-type enzyme (32.2 ± 3.5 1/min) with the enzymatic activity of the light- and dark-adapted state of the Q48E mutant being the same (Figure 5(B)).

In the dark, the Q48E mutant shows significant cAMP production compared to the wild-type enzyme, in which the basal activity is reported to be very low.[4,46] Turning on the laser at 150 s did not result to an increase of the cAMP production (Figure S4).

The results of the enzymatic assays are summarized in Table 1. These findings suggest that although the Q48E mutant is not photoactive (consistent with the absence of the characteristic red-shift in the absorption spectrum upon blue-light illumination), it has the ability to convert continuously and at a higher rate ATP to cAMP than wild-type OaPAC. This suggests that the Q48E mutation induces a conformational change in OaPAC that favours the ATP conversion but suppresses the light-induced changes in the hydrogen bond network of the flavin.Table 2..

Table 1 Frequencies measured by transient infrared absorption and the assignment of the respective peaks.

Frequency	Assignment
1420 (+)	FAD*[17]
1512 (+)	Tyr•[45]
1533 (+)	FADH•[55]
1547 (–)	FAD[29–31,56–57]
1690 (–)	FAD C4 = O light adapted state[22,30]
1704 (–)	FAD C4 = O dark adapted state[22,30]
1704 (+)	E48 (C = O)
1730 (–)	E48 (C = O)[22,58]

Differential scanning calorimetry (DSC) measurements

As the enzymatic activity of OaPAC changes with the Q48E mutation, suggesting a change in the protein structure, we performed differential scanning calorimetry measurements to examine the thermostability of the mutant. Figure 6 shows the heat-flux DSC curves for the wild-type and the Q48E OaPAC in which the melting temperature (T_m) shows where 50% of the protein is denatured whereas the area under the curve reflects the energy required for protein unfolding associated with the enthalpy change (ΔH). The measurements reveal significant differences between the wild-type and the mutant OaPAC. In particular, the thermal denaturation of the wild-type OaPAC shows a steep endothermic unfolding with a T_m of 68.0 °C and a ΔH of 0.078 ± 0.005 J/g. The T_m of the Q48E OaPAC is significantly lower (*T*m 63.6 °C) but there is no significant change in the enthalpy of unfolding ΔH of 0.072 ± 0.005 J/g. The lower melting temperature suggests a less compact and more flexible conformation for the Q48E mutant which seem to result to an increased

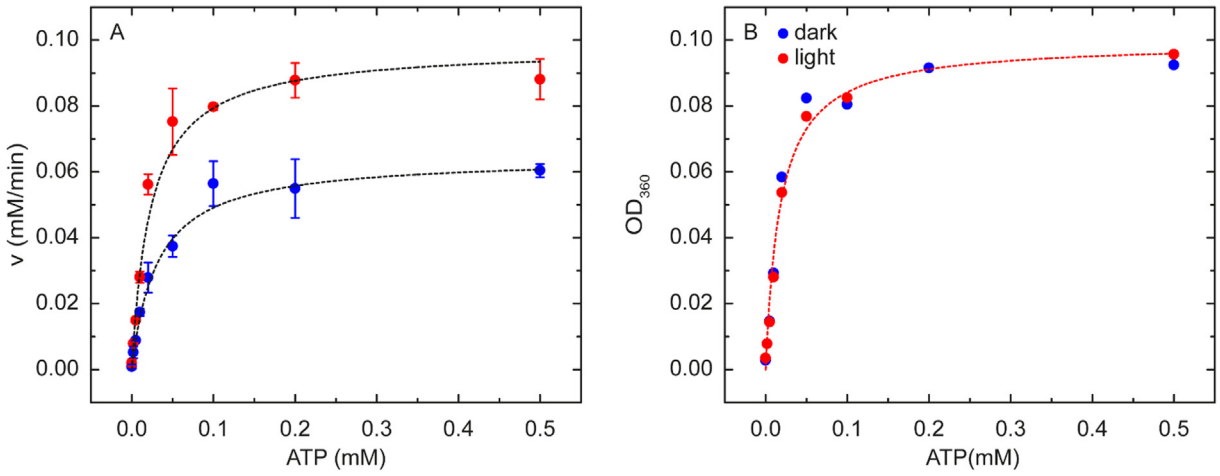

Figure 5. A) Michaelis-Menten plot of the enzymatic activity of WT (blue circles) and Q48E (red circles) under irradiation. B) Michaelis-Menten plot of the enzymatic activity of Q48E without irradiation (blue circles) and under irradiation (red circles) (the dashed line is the obtained fit). The plot shows that the mutant is in a "switched on" state as light irradiation does not affect the enzymatic activity.

Table 2 Enzymatic parameters of light adapted state of WT OaPAC and Q48E in dark and light state.

Kinetic parameters	WT (light)	Q48E dark	Q48E light
v_{max} (mM min^{-1})	0.064 ± 0.001	0.099 ± 0.004	0.101 ± 0.004
k_{cat} (min^{-1})	32.2 ± 3. 5	49.5 ± 2	50.5 ± 2
K_M (mM)	0.031 ± 0.001	0.018 ± 0.003	0.021 ± 0.002

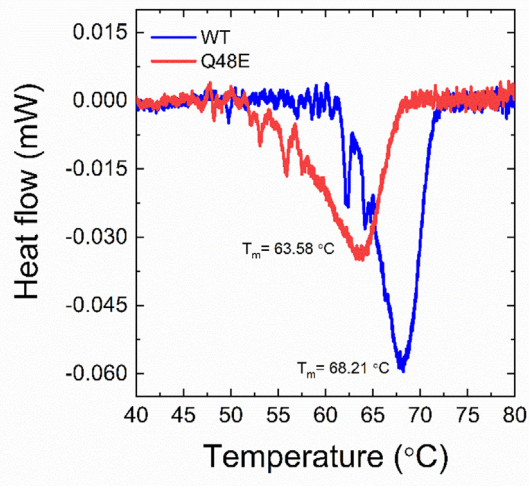

Figure 6. Thermal unfolding of wild-type OaPAC and Q48E OaPAC mutant measured by DSC.

cAMP production compared to the wild-type OaPAC.

Conclusions

In BLUF domains the functional role of the glutamine residue close to the N5 atom of the flavin has been investigated extensively, as the mutation of this amino acid in all known BLUF proteins results in a loss of the photoactivity[16,21] as well as due to the generally accepted scheme that photoactivation in all BLUF domains happens via the tautomerisation of this glutamine.[16,22,34,36,59–61]

The implications of the replacement of this crucial glutamine was investigated first in AppA, another BLUF domain protein, by means of transient ultrafast infrared spectroscopy in the case of the Q63L mutant.[16] TRIR measurements established that in this specific mutant the hydrogen network does not undergo a reorganization during the photoactivation. The C4 = O carbonyl peak of the Q63L mutant does not shift after excitation compared the to the well-established picture seen in the photoactive BLUF domain where this carbonyl peak shifts from ~1705 nm down to 1685–1690 nm pointing to hydrogen bond formation with C4 = O.[16,30] After these measurements Dragnea et al.[21] made the Q63E mutant and based on UV/VIS and fluorescence spectroscopy measurements proposed that this mutant is in a lit state. Our TRIR measurements using ^{13}C labelling showed that glutamic acid (E63) forms a hydrogen bond with the C4 = O carbonyl of flavin either before or together with the excitation[22] resulting in the downshift of the carbonyl peak in the same way as was observed for the light adapted state of AppA.[30] Dragnea et al. using size exclusion chromatography observed that the AppA Q63E mutant does not form a complex with PpsR.[21] As the common understanding was that AppA and PpsR form a complex in the dark and low oxygen levels but dissociate upon blue light irradiation the authors proposed that AppA Q63E adapts a structure which keeps the protein in a lit state. This picture was questioned by the finding of the Schlichting group who observed that the AppA-PpsR complex does not dissociate upon light irradiation.[62] After the discovery of OaPAC, a photoactivated adenylate cyclase we revisited the role of the mentioned glutamine as this special BLUF domain protein contains both sensor domain and the effector domain. In this way we were able to observe the effect of the site directed mutagenesis on the function of the protein directly.

Replacement of glutamine with glutamic acid in OaPAC resulted in very similar TRIR spectra to AppA Q63E and based on the assignment of the peaks we can conclude the following scheme (Figure 7): the glutamic acid forms two hydrogen bond with the flavin, one at N5 and one at C4 hence, on excitation we observe the vibration of the carbonyl of the protonated glutamic acid side chain (1730 cm^{-1}) as well as the vibrational mode of the C4 = O carbonyl (~1690 cm^{-1}); this latter is downshifted compared to the frequency observed in wild type (1704 cm^{-1}). After excitation the tyrosine (Y6) gives an electron to the flavin and a proton to the glutamic acid – that might be the origin of the positive 1704 cm^{-1} peak – and the glutamic acid gives a proton to the flavin (Grotthus-like mechanism). Observing the individual kinetics at 1533 and 1704 cm^{-1} we propose that the protonation of the glutamic acid and the flavin happens within the same time constant (~33 ps). The individual kinetic data (at 1533 cm^{-1} and 1704 cm^{-1}) as well as the EAS3 show that the proton and the electron is transferred back in 346 ps and the flavin relaxes back to it's original (lit) state.

The structural change caused by the Q48 → E48 mutation is reflected in the UV/VIS and calorimetry experiments as well. These latter have shown that the Q48E mutation results in a less compact structure, possibly by inducing a structural change

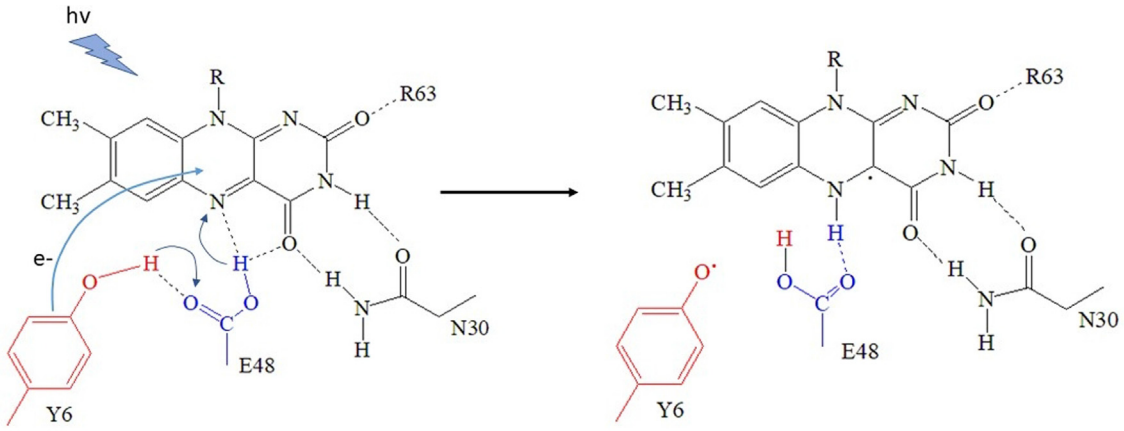

Figure 7. Photochemistry of flavin and surrounding amino acid due to light absorption. After blue light excitation an electron transferred to the flavin and a proton to the glutamic acid in concerted way. A proton is transferred within the same time constant to the flavin and the neutral flavin radical is stabilized.

in the enzyme as indicated by the ~5 °C drop of the melting temperature compared to the wild-type OaPAC. These observations suggest that the change in the hydrogen network around the flavin (seen in the UV/Vis and the infrared spectra) induces a larger structural change. Enzymatic activity assays have proved that this structural change has a substantial impact on the function of the enzyme as it converts ATP to cAMP in a light independent manner. Replacement of glutamine to glutamic acid resulted in the decoupling of the BLUF domain from AC domain of the protein.

Experimental

Materials and methods

Expression and purification of full-length Q48E mutant OaPAC. The wild type and Q48E mutant OaPAC sequences were normalized and purchased from GenScript. The sequences were inserted into a pET-15b vector in frame with an N-terminal His6-tag under control of a T7 promoter.

The purification of proteins were described earlier[63] with some minor changes. Briefly, protein expression was performed using freshly transformed BL21(DE3) cells. 10 ml Luria broth (LB) medium containing 10 mg/mL ampicillin was inoculated with a single colony and incubated at 37 °C overnight then used to inoculate 1 L of LB/ampicillin medium in a 4-L flask. The protein expression was induced when OD600 reached 0.4–0.6 with the addition of 0.7 mM IPTG at 18 °C. The harvested and frozen cell pellet was resuspended in 4x volume lysis buffer with 0.2 mM phenylmethylsulfonyl fluoride (PMSF), DNase, protease inhibitor cocktail, and lysozyme. The cells were lysed by sonication and cell debris was removed by centrifugation (12,000 rcf, 1 h). The supernatant was loaded onto a Ni-NTA (Qiagen) column and incubated it for 1 h at 4 °C followed by the elution of protein using 300 mM imidazole. The eluted protein was dialyzed, and purified to homogeneity using size-exclusion chromatography (Superdex-200).

The following buffers were used: lysis buffer (50 mM Na-phosphate buffer, 300 mM NaCl, pH 8.0), wash buffer (50 mM Na-phosphate buffer, 300 mM NaCl, 5 mM imidazole, pH 8.0) elution buffer (50 mM Na-phosphate buffer, 300 mM NaCl, 300 mM imidazole, pH 8.0), dialysis buffer (50 mM Tris, 150 mM NaCl, 5 mM MgCl2 pH 8.0).

Transient infrared spectroscopy (TRIR)

TRIR spectra were obtained at 20 °C from 100 fs to 3 ns on the ULTRA system at the STFC Central Laser Facility. The ULTRA system has been described elsewhere,[64] and previously used by us to analyse the photoactivation of AppABLUF,[22,30,55,65,33] and other photoactive and photochromic proteins.[66–67] Light sensitive samples were analysed using a rastered flow cell, and data were acquired using a 450 nm pump pulse operated at 0.2–0.4 μJ per pulse and a repetition rate of 5 kHz. The spectral resolution was 3 cm-1 and the temporal resolution was < 200 fs. All samples were prepared at 0.6–0.8 mM concentration in D_2O buffer prepared with 20 mM Tris, 150 mM NaCl, pD 8.0. TRIR data were globally analysed using Glotaran[68][assuming a sequential scheme with evolutionary associated difference spectra (EADS) assigned to the obtained time constants.[69]

Ultrafast transient absorption experiments

Ultrafast transient absorption measurements were performed using a Spitfire Ace regenerative amplifier system providing ~800 μJ pulses centered at 800 nm at a repetition rate of 1 kHz. The output of the amplifier was split in a ratio 1:9. The pulse with the smaller energy was used for

the generation of the white light continuum probe in a CaF2 crystal. The higher intensity fraction was frequency doubled to 400 nm and attenuated to ~200–400 nJ/pulse before being used as the pump pulse. Polarization of the probe was set to the magic angle compared to excitation. To avoid photodegradation the samples were moved with the help of a Lissajous scanner and simultaneously flowed by a peristaltic pump. Absorption changes were measured with an Andor CCD and collected with the help of a home written Labview data acquisition software, and are reported as pump on – pump off normalized difference spectra. The transient absorption dataset was also globally analysed using the Java based software package Glotaran.[68]

cAMP yield measurement / adenylate cyclase activity

The ATP-cAMP conversion of the wild-type and the Q48E OaPAC mutant was quantified using a pyrophosphate (PPi) assay (EnzChek® Pyrophosphate Assay Kit). The assay is based on the PPi-dependent conversion of the 2-amino-6-mercapto-7-methylpurine ribonucleoside (MESG) to ribose 1-phosphate and 2-amino-6-mercapto-7-methylpurine by the enzyme purine nucleoside phosphorylase (PNP). The enzymatic conversion of MESG results in a shift in absorbance maximum from 330 to 360 nm. In addition, the PPi originating from the conversion of ATP to cAMP is catalysed to two equivalents of phosphate by the enzyme inorganic pyrophosphate present in the assay and enhancing this way the sensitivity as the phosphate is consumed by the MESG/PNP reaction and the product of the production is detected by an increase in the absorbance at 360 nm. The increase of the absorption at 360 nm was monitored as a function of time. The reaction rate was determined from the slope of a linear fit using an extinction coefficient of 11,000 $M^{-1}cm^{-1}$ at 360 nm.

The adenylate cyclase activity of 2 μM of WT and Q48E mutant OaPAC was monitored by continuous illumination with a 473 nm laser light adjusted to a power of 9 mW in the absence and presence of 500 μM of ATP. The reaction rate (μM/s) was determined from the slope of the absorbance of the purine base product (2-amino-6-mercapto-7-m ethypurine), which is equal to the reaction rate of pyrophosphate derived from ATP cyclization.

To determine the Michaelis-Menten constant, the assay was performed on WT OaPAC and the Q48E mutant in the presence of 0–500 μM concentrations of ATP using the same conditions of continuous illumination. The initial reaction rate at each ATP concentration was extracted from the linear portion of OD_{360} vs. time plot. The resulting rate constants were plotted as a function of ATP. By fitting a Michaelis-Menten saturation curve for the enzyme reaction, the maximum reaction rate (V_{max}) and the corresponding K_M were determined.

Differential scanning calorimetry (DSC) measurements

Differential scanning calorimetry (DSC) was performed to measure the thermal stability of the WT and Q48E mutant OaPAC using a SETARAM Micro DSC-III calorimeter. The measurements were carried out in the range of 20 – 100 °C with a heating rate of 0.3 $K{\cdot}min^{-1}$. The sample (WT and Q48E) and the reference (buffer solution of WT and Q48E) were balanced with a precision of ± 0.05 mg in order to avoid corrections with the heat capacity of the vessels. A second thermal scan of the denatured sample was measured for baseline correction. The melting temperature (T_m) of the thermal unfolding curves were analyzed by the OriginLab Origin®2021 software.

Author Contributions

J.T.C., Z.F.,N.K.B. made the constructs, expressed and purified the proteins. A.L., J.T.C, G.G performed the infrared transient absorption measurements; A.L., S.R.M., P.J.T. analysed the transient infrared data. E.B., J.P., M.S. performed the transient absorption measurements. E.B., designed, performed and analysed the cAMP assays. DSC experiments were performed and analysed by E.T., K.P.U. The project was conceived by S.R.M, S.M.K., A.L., P.J.T. The manuscript was written by E.B., S.M. K., S.R.M. and A.L.

CRediT authorship contribution statement

Jinnette Tolentino Collado: Investigation, Conceptualization. **Emoke Bodis:** Investigation. **Jonatan Pasitka:** Investigation. **Mihaly Szucs:** Investigation. **Zsuzsanna Fekete:** Investigation, Methodology. **Nikolett Kis-Bicskei:** Investigation, Methodology. **Elek Telek:** Investigation. **Kinga Pozsonyi:** Investigation. **Sofia M. Kapetanaki:** Conceptualization. **Greg Greetham:** Investigation. **Peter J. Tonge:** Conceptualization. **Stephen R. Meech:** Conceptualization. **Andras Lukacs:** Conceptualization, Investigation.

DECLARATION OF COMPETING INTEREST

The authors declare that they have no known competing financial interests or personal relationships that could have appeared to influence the work reported in this paper.

Acknowledgements

J.T.C. was supported by the National Institutes of Health IMSD-MERGE (T32GM135746) and NY-CAPs IRACDA (K12-GM102778) Programs at

Stony Brook University. A.L. acknowledges funding from the Hungarian National Research and Innovation Office (K-137557) and was supported by PTE ÁOK-KA-2021. E.T was supported by PTE ÁOK-KA-2022-09. This study was supported by the National Science Foundation (NSF) (MCB-1817837 to PJT) and the EPSRC (EP/N033647/1 to S.R.M.).

Appendix A. Supplementary data

Supplementary data to this article can be found online at https://doi.org/10.1016/j.jmb.2023.168312.

Received 23 June 2023;
Accepted 5 October 2023;
Available online 10 October 2023

Keywords:
structure;
chemistry;
processing and function of biologically important macromolecules and complexes

# Equally contributed.

References

1. Ohki, M., Sugiyama, K., Kawai, F., Matsunaga, S., Iseki, M., Park, S., (2016). Structural basis for photoactivation of a light-regulated adenylate cyclase from the photosynthetic cyanobacterium Oscillatoria acuminata. *Acta Crystallograph. a-Foundation Adv.* **72**, S251.
2. Iseki, M., Park, S.Y., (2021). Photoactivated adenylyl cyclases: fundamental properties and applications. *Adv. Exp. Med. Biol.* **1293**, 129–139.
3. Lindner, R., Hartmann, E., Tarnawski, M., Winkler, A., Frey, D., Reinstein, J., et al., (2017). Photoactivation mechanism of a bacterial light-regulated adenylyl cyclase. *J. Mol. Biol.* **429**, 1336–1351.
4. Collado, J., Iuliano, J., Pirisi, K., Jewlikar, S., Adamczyk, K., Greetham, G., et al., (2022). Unraveling the photoactivation mechanism of a light-activated adenylyl cyclase using ultrafast spectroscopy coupled with unnatural amino acid mutagenesis. *ACS Chem. Biol.* **17**, 2643–2654.
5. Lukacs, A., Tonge, P.J., Meech, S.R., (2022). Photophysics of the blue light using flavin domain. *Acc. Chem. Res.* **55**, 402–414.
6. Gauden, M., Yeremenko, S., Laan, W., van Stokkum, I., Ihalainen, J., van Grondelle, R., et al., (2005). Photocycle of the flavin-binding photoreceptor AppA, a bacterial transcriptional antirepressor of photosynthesis genes. *Biochemistry* **44**, 3653–3662.
7. Kennis, J.T., Groot, M.L., (2007). Ultrafast spectroscopy of biological photoreceptors. *Curr. Opin. Struct. Biol.* **17**, 623–630.
8. Fujisawa, T., Masuda, S., (2018). Light-induced chromophore and protein responses and mechanical signal transduction of BLUF proteins. *Biophys. Rev.* **10**, 327–337.
9. Jung, A., Reinstein, J., Domratcheva, T., Shoeman, R.L., Schlichting, I., (2006). Crystal structures of the AppA BLUF domain photoreceptor provide insights into blue light-mediated signal transduction. *J. Mol. Biol.* **362**, 717–732.
10. Jung, A., Domratcheva, T., Tarutina, M., Wu, Q., Ko, W.H., Shoeman, R.L., et al., (2005). Structure of a bacterial BLUF photoreceptor: insights into blue light-mediated signal transduction. *PNAS* **102**, 12350–12355.
11. Brust, R., Lukacs, A., Haigney, A., Addison, K., Gil, A., Towrie, M., et al., (2013). Proteins in action: femtosecond to millisecond structural dynamics of a photoactive flavoprotein. *J. Am. Chem. Soc.* **135**, 16168–16174.
12. Gauden, M., Grinstead, J., Laan, W., van Stokkum, I., Avila-Perez, M., Toh, K., et al., (2007). On the role of aromatic side chains in the photoactivation of BLUF domains. *Biochemistry* **46**, 7405–7415.
13. Bonetti, C., Mathes, T., van Stokkum, I.H., Mullen, K.M., Groot, M.L., van Grondelle, R., et al., (2008). Hydrogen bond switching among flavin and amino acid side chains in the BLUF photoreceptor observed by ultrafast infrared spectroscopy. *Biophys. J* . **95**, 4790–4802.
14. Bonetti, C., Stierl, M., Mathes, T., van Stokkum, I., Mullen, K., Cohen-Stuart, T., et al., (2009). The role of key amino acids in the photoactivation pathway of the synechocystis Slr1694 BLUF domain. *Biochemistry* **48**, 11458–11469.
15. Stierl, M., Penzkofer, A., Kennis, J., Hegemann, P., Mathes, T., (2014). Key residues for the light regulation of the blue light-activated adenylyl cyclase from Beggiatoa sp. *Biochemistry* **53**, 5121–5130.
16. Stelling, A.L., Ronayne, K.L., Nappa, J., Tonge, P.J., Meech, S.R., (2007). Ultrafast structural dynamics in BLUF domains: transient infrared spectroscopy of AppA and its mutants. *J. Am. Chem. Soc.* **129**, 15556–15564.
17. Lukacs, A., Brust, R., Haigney, A., Laptenok, S.P., Addison, K., Gil, A., et al., (2014). BLUF domain function does not require a metastable radical intermediate state. *J. Am. Chem. Soc.* **136**, 4605–4615.
18. Okajima, K., Fukushima, Y., Suzuki, H., Kita, A., Ochiai, Y., Katayama, M., et al., (2006). Fate determination of the flavin photoreceptions in the cyanobacterial blue light receptor TePixD (Tll0078). *J. Mol. Biol.* **363**, 10–18.
19. Fukushima, Y., Murai, Y., Okajima, K., Ikeuchi, M., Itoh, S., (2008). Photoreactions of Tyr8- and Gln50-mutated BLUF domains of the PixD protein of Thermosynechococcus elongatus BP-1: photoconversion at low temperature without Tyr8. *Biochemistry* **47**, 660–669.
20. Yuan, H., Anderson, S., Masuda, S., Dragnea, V., Moffat, K., Bauer, C., (2006). Crystal structures of the Synechocystis photoreceptor Slr1694 reveal distinct structural states related to signaling. *Biochemistry* **45**, 12687–12694.
21. Dragnea, V., Arunkumar, A., Lee, C., Giedroc, D., Bauer, C., (2010). A Q63E Rhodobacter sphaeroides AppA BLUF Domain Mutant Is Locked in a Pseudo-Light-Excited Signaling State. *Biochemistry* **49**, 10682–10690.
22. Lukacs, A., Haigney, A., Brust, R., Zhao, R.K., Stelling, A. L., Clark, I.P., et al., (2011). Photoexcitation of the blue light using FAD photoreceptor AppA results in ultrafast changes to the protein matrix. *J. Am. Chem. Soc.* **133**, 16893–16900.
23. Anderson, S., Dragnea, V., Masuda, S., Ybe, J., Moffat, K., Bauer, C., (2005). Structure of a novel photoreceptor, the BLUF domain of AppA from Rhodobacter sphaeroides. *Biochemistry* **44**, 7998–8005.

24. I S. infrared spectra and normal vibrations of acetamide and its deuterated analogues. Bull. Chem. Soc. Jpn. 1962;35:1279–1286.
25. Sayfutyarova, E., Goings, J., Hammes-Schiffer, S., (2019). Electron-coupled double proton transfer in the Slr1694 BLUF photoreceptor: a multireference electronic structure study. *J. Phys. Chem. B* **123**, 439–447.
26. Goings, J., Hammes-Schiffer, S., (2019). Early photocycle of Slr1694 blue-light using flavin photoreceptor unraveled through adiabatic excited-state quantum mechanical/molecular mechanical dynamics. *J. Am. Chem. Soc.* **141**, 20470–20479.
27. Gil, A.A., Laptenok, S.P., Iuliano, J.N., Lukacs, A., Verma, A., Hall, C.R., et al., (2017). Photoactivation of the BLUF protein PixD probed by the site-specific incorporation of fluorotyrosine residues. *J. Am. Chem. Soc.* **139**, 14638–14648.
28. Karadi, K., Kapetanaki, S.M., Raics, K., Pecsi, I., Kapronczai, R., Fekete, Z., et al., (2020). Functional dynamics of a single tryptophan residue in a BLUF protein revealed by fluorescence spectroscopy. *Sci. Rep.* **10**, 2061.
29. Kondo, M., Nappa, J., Ronayne, K., Stelling, A., Tonge, P., Meech, S., (2006). Ultrafast vibrational spectroscopy of the flavin chromophore. *J. Phys. Chem. B* **110**, 20107–20110.
30. Haigney, A., Lukacs, A., Zhao, R.K., Stelling, A.L., Brust, R., Kim, R.R., et al., (2011). Ultrafast infrared spectroscopy of an isotope-labeled photoactivatable flavoprotein. *Biochemistry* **50**, 1321–1328.
31. Wolf, M.M., Schumann, C., Gross, R., Domratcheva, T., Diller, R., (2008). Ultrafast infrared spectroscopy of riboflavin: dynamics, electronic structure, and vibrational mode analysis. *J. Phys. Chem. B* **112**, 13424–13432.
32. Wolf, M.M., Zimmermann, H., Diller, R., Domratcheva, T., (2011). Vibrational mode analysis of isotope-labeled electronically excited riboflavin. *J. Phys. Chem. B* **115**, 7621–7628.
33. Haigney, A., Lukacs, A., Brust, R., Zhao, R.K., Towrie, M., Greetham, G.M., et al., (2012). Vibrational assignment of the ultrafast infrared spectrum of the photoactivatable flavoprotein AppA. *J. Phys. Chem. B* **116**, 10722–10729.
34. Hontani, Y., Mehlhorn, J., Domratcheva, T., Beck, S., Kloz, M., Hegemann, P., et al., (2023). Spectroscopic and computational observation of glutamine tautomerization in the blue light sensing using flavin domain photoreaction. *J. Am. Chem. Soc.* **145**, 1040–1052.
35. Gauden, M., van Stokkum, I., Key, J., Luhrs, D., Van Grondelle, R., Hegemann, P., et al., (2006). Hydrogen-bond switching through a radical pair mechanism in a flavin-binding photoreceptor. *PNAS* **103**, 10895–10900.
36. Sadeghian, K., Bocola, M., Schütz, M., (2008). A conclusive mechanism of the photoinduced reaction cascade in blue light using flavin photoreceptors. *J. Am. Chem. Soc.* **130**, 12501–12513.
37. Chen, Z., Kang, X.W., Zhou, Y., Zhou, Z., Tang, S., Zou, S., et al., (2023). Dissecting the Ultrafast Stepwise Bidirectional Proton Relay in a Blue-Light Photoreceptor. *J. Am. Chem. Soc.* **145**, 3394–3400.
38. Agmon, N., (1995). The Grotthuss mechanism. *Chem. Phys. Lett.* **244**, 456–462.
39. Sun, M., Moore, T.A., Song, P.S., (1972). Molecular luminescence studies of flavins. I. The excited states of flavins. *J. Am. Chem. Soc.* **94**, 1730–1740.
40. Konold, P.E., Arik, E., Weißenborn, J., Arents, J.C., Hellingwerf, K.J., van Stokkum, I.H.M., et al., (2020). Confinement in crystal lattice alters entire photocycle pathway of the Photoactive Yellow Protein. *Nature Commun.* **11**, 4248.
41. Tonge, P., Moore, G., Wharton, C., (1989). Fourier-transform infrared studies of the alkaline isomerization of mitochondrial cytochrome-c and the ionization of carboxylic-acids. *Biochem. J* **258**, 599–605.
42. Fahmy, K., Jager, F., Beck, M., Zvyaga, T., Sakmar, T., Siebert, F., (1993). Protonation states of membrane-embedded carboxylic-acid groups in rhodopsin and metarhodopsin-II – a Fourier-transform infrared-spectroscopy study of site-directed mutants. *PNAS* **90**, 10206–10210.
43. Lubben, M., Gerwert, K., (1996). Redox FTIR difference spectroscopy using caged electrons reveals contributions of carboxyl groups to the catalytic mechanism of haem-copper oxidases. *FEBS Letter* **397**, 303–307.
44. Dioumaev, A., (2001). Infrared methods for monitoring the protonation state of carboxylic amino acids in the photocycle of bacteriorhodopsin. *Biochemistry-Moscow.* **66**, 1269–1276.
45. Pirisi, K., Nag, L., Fekete, Z., Iuliano, J.N., Tolentino Collado, J., Clark, I.P., et al., (2021). Identification of the vibrational marker of tyrosine cation radical using ultrafast transient infrared spectroscopy of flavoprotein systems. *Photochem. Photobiol. Sci.* **20**, 369–378.
46. Ohki, M., Sugiyama, K., Kawai, F., Tanaka, H., Nihei, Y., Unzai, S., et al., (2016). Structural insight into photoactivation of an adenylate cyclase from a photosynthetic cyanobacterium. *PNAS* **113**, 6659–6664.
47. Zhou, Z., Chen, Z., Kang, X.W., Zhou, Y., Wang, B., Tang, S., et al., (2022). The nature of proton-coupled electron transfer in a blue light using flavin domain. *Proc. Natl. Acad. Sci. USA* **119**
48. Dixon, W., Murphy, D., (1976). Determination of acidity constants of some phenol radical cations by means of electron-spin resonance. *J. Chem. Soc.-Faraday Trans. II* **72**, 1221–1230.
49. Solar, S., Gtoff, N., Surdhar, P.S., Armstrong, D.A., Singh, A., (1991). Oxidation of tryptophan and N-methylindole by N3•, Br 2•- and (SCN)2•- radicals in light- and heavy-water solutions: a pulse radiolysis study. *J. Phys. Chem.*, 3639–3643.
50. Nag, L., Sournia, P., Myllykallio, H., Liebl, U., Vos, M., (2017). Identification of the TyrOH(center dot+) radical cation in the flavoenzyme TrmFO (vol 139, pg 11500, 2017). *J. Am. Chem. Soc.* **139**, 15554.
51. Nag, L., Lukacs, A., Vos, M.H., (2019). Short-Lived Radical Intermediates in the Photochemistry of Glucose Oxidase. *ChemPhysChem* **20**, 1793–1798.
52. Pirisi, K., Nag, L., Fekete, Z., Iuliano, J.N., Collado, J.T., Clark, I.P., et al., (2021). Identification of the vibrational marker of tyrosine cation radical using ultrafast transient infrared spectroscopy of flavoprotein systems. *Photochem. Photobiol. Sci.* **20**, 369–378.
53. Green, D., Roy, P., Hall, C.R., Iuliano, J.N., Jones, G.A., Lukacs, A., et al., (2021). Excited State Resonance Raman of Flavin Mononucleotide: Comparison of Theory and Experiment. *Chem. A Eur. J.* **125**, 6171–6179.
54. Goings, J.J., Reinhardt, C.R., Hammes-Schiffer, S., (2018). Propensity for Proton Relay and Electrostatic

Impact of Protein Reorganization in Slr1694 BLUF Photoreceptor. *J. Am. Chem. Soc.* **140**, 15241–15251.
55. Lukacs, A., Zhao, R.K., Haigney, A., Brust, R., Greetham, G.M., Towrie, M., et al., (2012). Excited state structure and dynamics of the neutral and anionic flavin radical revealed by ultrafast transient mid-IR to visible spectroscopy. *J. Phys. Chem. B* **116**, 5810–5818.
56. Haigney, A., Kondo, M., Stelling, A., Lukacs, A., Bacher, A., Tonge, P., et al., (2010). Determining Structural Differences in the Dark and Light States of AppA using Vibrational and Ultrafast Fluorescence Spectroscopy. *FASEB J.* **24**
57. Zhu, J., Mathes, T., Stahl, A.D., Kennis, J.T., Groot, M.L., (2012). Ultrafast mid-infrared spectroscopy by chirped pulse upconversion in 1800–1000cm(-1) region. *Opt. Express* **20**, 10562–10571.
58. Hense, A., Herman, E., Oldemeyer, S., Kottke, T., (2015). Proton Transfer to Flavin Stabilizes the Signaling State of the Blue Light Receptor Plant Cryptochrome. *J. Biol. Chem.* **290**, 1743–1751.
59. Khrenova, M.G., Domratcheva, T., Schlichting, I., Grigorenko, B.L., Nemukhin, A.V., (2011). Computational characterization of reaction intermediates in the photocycle of the sensory domain of the AppA blue light photoreceptor. *Photochem. Photobiol.* **87**, 564–573.
60. Khrenova, M.G., Nemukhin, A.V., Domratcheva, T., (2013). Photoinduced electron transfer facilitates tautomerization of the conserved signaling glutamine side chain in BLUF protein light sensors. *J. Phys. Chem. B* **117**, 2369–2377.
61. Hsiao, Y.W., Götze, J.P., Thiel, W., (2012). The central role of Gln63 for the hydrogen bonding network and UV-visible spectrum of the AppA BLUF domain. *J. Phys. Chem. B* **116**, 8064–8073.
62. Winkler, A., Heintz, U., Lindner, R., Reinstein, J., Shoeman, R.L., Schlichting, I., (2013). A ternary AppA-PpsR-DNA complex mediates light regulation of photosynthesis-related gene expression. *Nature Struct. Mol. Biol.* **20**, 859–867.
63. Kapetanaki, S.M., Fekete, Z., Dorlet, P., Vos, M.H., Liebl, U., Lukacs, A., (2022). Molecular insights into the role of heme in the transcriptional regulatory system AppA/PpsR. *Biophys. J* . **121**, 2135–2151.
64. Greetham, G., Burgos, P., Cao, Q., Clark, I., Codd, P., Farrow, R., et al., (2010). ULTRA: A unique instrument for time-resolved spectroscopy. *Appl. Spectrosc.* **64**, 1311–1319.
65. Zhao, R.K., Lukacs, A., Haigney, A., Brust, R., Greetham, G.M., Towrie, M., et al., (2011). Ultrafast transient mid IR to visible spectroscopy of fully reduced flavins. *PCCP* **13**, 17642–17648.
66. Lukacs, A., Haigney, A., Brust, R., Addison, K., Towrie, M., Greetham, G.M., et al., (2013). Protein photochromism observed by ultrafast vibrational spectroscopy. *J. Phys. Chem. B* **117**, 11954–11959.
67. Laptenok, S.P., Lukacs, A., Gil, A., Brust, R., Sazanovich, I.V., Greetham, G.M., et al., (2015). Complete proton transfer cycle in GFP and Its T203V and S205V mutants. *Angew. Chem. Int. Ed. Engl.* **54**, 9303–9307.
68. Snellenburg, J., Laptenok, S., Seger, R., Mullen, K., van Stokkum, I., (2012). Glotaran: a Java-Based Graphical User Interface for the R Package TIMP. *J. Stat. Softw.* **49**, 1–22.
69. van Stokkum, I.H., Larsen, D.S., van Grondelle, R., (2004). Global and target analysis of time-resolved spectra. *BBA* **1657**, 82–104.